

## Supporting Information

### Nanosurfacing Ti alloy by weak alkalinity-activated solid-state dewetting (AAD) and its biointerfacial enhancement effect

*Xiaoxia Song<sup>1#</sup>, Fuwei Liu<sup>2#</sup>, Caijie Qiu<sup>1</sup>, Emerson Coy<sup>3</sup>, Hui Liu<sup>1</sup>, Willian Aperador<sup>4</sup>, Karol Załęski<sup>3</sup>, Jiao Jiao Li<sup>5</sup>, Wen Song<sup>2</sup>, Zufu Lu<sup>6</sup>, Haobo Pan<sup>1</sup>, Liang Kong<sup>2\*</sup>, Guocheng Wang<sup>1\*</sup>*

---

<sup>1</sup>Research Center for Human Tissues & Organs Degeneration, Shenzhen Institute of Advanced Technology, Chinese Academy of Science, Shenzhen, Guangdong 518055, China

E-mail: [gc.wang@siat.ac.cn](mailto:gc.wang@siat.ac.cn)

<sup>2</sup>State Key Laboratory of Military Stomatology & National Clinical Research Center for Oral Diseases and Shaanxi Clinical Research Center for Oral Diseases, Department of Oral and Maxillofacial Surgery, School of Stomatology, The Fourth Military Medical University, Xi'an, 710032, China

Email: [liangkong2014@163.com](mailto:liangkong2014@163.com)

<sup>3</sup>NanoBioMedical Centre, Adam Mickiewicz University, Wszechnicy Piastowskiej 3, 61614 Poznań, Poland

<sup>4</sup>School of Engineering, Universidad Militar Nueva Granada, Carrera 11 #101-80, 49300 Bogotá, Colombia

<sup>5</sup>School of Biomedical Engineering, Faculty of Engineering and IT, University of Technology Sydney (UTS), NSW 2007, Australia

<sup>6</sup>Biomaterials and Tissue Engineering Research Unit, University of Sydney, Darlington 2006, Australia

## 1. Materials and Methods

### 1.1 Materials

Biomedical grade Ti6Al4V discs with a diameter of 15mm and thickness of 1mm were commercially obtained (Baoji Junhang Metal Material Co., Ltd. Shanxi, China). Prior to use in any procedure, the discs were pre-washed with a diluted acid solution containing 20mL pure water (H<sub>2</sub>O), 0.02mL 48 % hydrofluoric acid (HF), and 0.13mL 48% nitric acid (HNO<sub>3</sub>), followed by ultrasonic wash with milli-Q water.

### 1.2 Weak alkalinity-activated solid-state dewetting (AAD)

Briefly, pre-washed Ti6Al4V discs were placed in a tubular container containing 4M ammonia phosphate dibasic (APD; (NH<sub>4</sub>)<sub>2</sub>HPO<sub>4</sub>) solution and treated at 60 °C for 4 h. The samples were

then placed in a furnace and thermally oxidized in air at 500 °C for 1 h. These samples subjected to both APD and heat treatment were denoted Ti-4M-H. For comparing the effects of APD treatment on the formation of nanotopographic features on the Ti alloy, control groups were prepared consisting of untreated Ti alloy (Ti group) and Ti alloy subjected to heat treatment only at 500 °C for 1 h (Ti-H group).

### 1.3 Characterization

To characterize the crystalline structure and chemical composition of nanograins in Ti-H and Ti-4M-H, grazing incident X-ray diffraction (GIXRD, PANalytical, Netherlands) with an incident angle of 1° and data in the range of 2theta from 20 to 80° were collected. Data analysis was performed using the X'pert HighScore Plus software (PANalytical). X-ray photoelectron spectroscopy (XPS) was performed using a SPECS Sage HR 100 spectrometer with a non-monochromatic aluminum X-ray source ( $K\alpha$ , 1486.6 eV). Samples were placed perpendicular to the analyzer. The selected resolution for the high resolution spectra was 1.1 eV, measured on a clean silver surface and defined as the full width at half maximum (FWHM) of the Ag 3d<sub>5/2</sub> peak. The parameters used to obtain this resolution were 10 eV of Pass Energy, 0.15 eV/step and source power of 300 W. Measurements were made in an ultra-high vacuum (UHV) chamber at a pressure of  $5 \times 10^{-6}$  Pa. Asymmetric and Gaussian Lorentzian functions were used for spectra fitting after a Shirley background correction, by which the FWHM of all peaks were constrained while the peak positions and areas were set free.

The surface morphology of discs was examined by scanning electron microscopy (SEM; ZEISS SUPRA®55, Carl Zeiss, Germany) and atomic force microscopy (AFM; Nanoscope V, Bruker, USA). For AFM imaging, contact mode using oxide-sharpened silicon nitride tips was applied, and information was collected on an area of  $1 \times 1 \mu\text{m}$ . The surface chemical composition of

discs was examined using an energy dispersive X-ray (EDX) detector (JSM-5900LV, Joel Ltd., Tokyo, Japan).

Contact angles were measured by static contact angle using the sessile drop method (Contact Angle System HARRE-SPCA, China). Ultrapure water (Millipore Milli-Q, Merck Millipore Corporation, USA) and diiodomethane were used as working fluids. Measurements were performed in triplicate at room temperature, with an initial volume of 3  $\mu\text{L}$  and a dose rate of 1  $\mu\text{L}/\text{min}$ . The surface energy (SE) and its dispersive/polar components were calculated using the Young–Laplace and Owen–Wendt equations, as previously reported [1–3]. Data was analyzed using SCA 20 software (Dataphysics).

#### 1.4 Tribo-corrosion tests

The test duration was guided by the average distance travelled by patients undergoing hip arthroplasty. To determine this distance, it was important to establish the sliding arch in the femoral head. The tests were performed at 37 °C in aerated Ringer physiological solution, composed of 9 g/L NaCl, 0.4 g/L KCl, 0.17 g/L  $\text{CaCl}_2$  and 2.1 g/L  $\text{NaHCO}_3$ . A constant load of 5 N was applied with an oscillation frequency of 1 Hz. The length travelled by the pin in each cycle was 10 mm, with the total time for each electrochemical test being 240 minutes. The average coefficient of friction ( $\mu$ ) and the wear coefficients of both the sphere and the coating were determined.

To study the influence of simultaneous abrasive wear and corrosion, a tribocorrosion test was performed using a T50 Nanovea tribometer at  $37 \pm 0.2$  °C (normal body temperature). The tribometer was an electrochemical cell consisting of a series of three electrodes: the reference (Ag/AgCl), the counter electrode (platinum wire), and a specimen with 1  $\text{cm}^2$  area of exposure. A Gamry potentiostat (Model No. PCI 4/750) was used for the evaluation of resistance to corrosion and wear. Tafel polarization curves were measured with a scanning rate of 0.125

mV/s, within a range of voltages from -400 mV to +1400 mV with respect to the corrosion potential ( $E_{\text{corr}}$ ). The values of corrosion current density ( $i_{\text{corr}}$ ) and corrosion potential ( $E_{\text{corr}}$ ) were obtained from the polarization curves by extrapolation of the cathodic and anodic branches to the corrosion potential. All electrochemical measurements were repeated at least three times.

## 1.5 In vitro assay for evaluation of osteoblast activities

### 1.5.1 MC3T3-E1 culture

A murine pre-osteoblast cell line (MC3T3-E1) was used for *in vitro* evaluation of Ti-4M-H compared to Ti and Ti-H. Briefly, cells were cultured using growth medium consisting of  $\alpha$ -MEM supplemented with 10% fetal bovine serum (FBS) and 1% penicillin/streptomycin, at 37 °C and 5% CO<sub>2</sub> in a humidified environment. The samples were sterilized by autoclaving at 121 °C for 20 min, and placed in 24-well tissue culture plates for cell seeding. Cells were seeded by dropping 1 mL of cell suspension at a density of  $2 \times 10^4$  cells/mL onto each sample.

### 1.5.2 Scratch migration assay

Migration was determined using a scratch wound healing assay according to a published protocol [4]. Briefly, MC3T3-E1 cells were seeded onto samples in 24-well plates at a density of  $1 \times 10^6$  cells/well and allowed to reach confluence. A 200  $\mu$ L pipette tip was used to make a scratch across the cell monolayer. The cells were washed with PBS and fresh growth medium was added. Regions of interest were imaged every 30 min using SEM.

### 1.5.3 Cell viability and cell proliferation

The cell viability Kit-8 (CCK-8 assay, Beyotime, China) was used to quantitatively determine the cytotoxicity of samples. MC3T3-E1 cells were seeded onto samples in 24-well plates at a density of  $2 \times 10^4$  cells/well, and cultured in growth medium for 1, 3 and 7 days. At each time point, 10% CCK-8 solution in culture medium was added and incubated at 37 °C for 2 h. The

optical density values were read at 450 nm using a multifunctional full wavelength microplate reader (Multiskan GO, Thermo Fisher Scientific, USA).

#### 1.5.4 Mineralization assay

The extent of extracellular matrix mineralization after 21 days of culturing was visualized by Alizarin Red S and Sirius Red staining. For Alizarin Red S staining, after fixation for 15 min in 2.5% glutaraldehyde solution, samples were stained using ARS (1%, pH 4.3). For Sirius Red staining, 0.1% (w/v) Sirius Red in saturated picric acid were added after fixation. Pictures were photographed using fluorescence microscopy (OLYMPUS BX53, Japan). ARS Stain quantification was performed by eluting using a 10% cetylpyridinium chloride solution for 30min. Optical density was measured at 540 nm using 50  $\mu$ L of eluent. Sirius Red Stain quantification, dyes were washed with 0.2 M sodium hydroxide/methanol mixture (1:1) and measured on a microplate reader at 590 nm. All materials were from Sigma Aldrich, USA.

#### 1.5.5 Osteogenic gene expression of MC3T3-E1 cells

Cells were seeded onto samples in a 24-well plate at an initial density of  $1 \times 10^5$  cells/well. After incubation for 24 h in growth medium, the medium was replaced by osteogenic differentiation medium consisting of  $\alpha$ -MEM supplemented with 10% FBS, 10 mM  $\beta$ -glycerophosphate, 50 mg/mL ascorbic acid and 0.1 mM dexamethasone. At 3 and 7 days, total RNA in the cells was extracted using Trizol reagent (Takara, Japan) according to the manufacturer's instructions. RNA concentration was quantified using a NanoDrop spectrophotometer (Thermo, USA). Complementary DNA (cDNA) was synthesized from 1  $\mu$ g RNA using a PrimeScript RT reagent kit (Takara, Japan) according to the manufacturer's instructions. Gene expression analysis was performed with a CFX96<sup>TM</sup> Real-Time PCR detection System (Bio-Rad, USA) using SYBR Premix Ex Taq<sup>TM</sup> (Takara, Japan). Cycle conditions were set as follows: denaturation at 95°C for 30 s; 40 cycles at 95°C for 5 s; and

60°C for 30 s; melt curve from 65°C to 95°C with increment of 0.5°C/5s. Osteogenic differentiation markers including runt-related transcription factor 2 (Runx2), osteopontin (OPN), osteocalcin (OCN), and alkaline phosphatase (ALP) were evaluated, which were normalised to GAPDH as a housekeeping gene. Cells cultured in wells without samples were used as the control. Data were analyzed using the comparative Ct ( $2^{-\Delta\Delta Ct}$ ) method and expressed as a fold change with respect to the control. All samples were assayed in triplicate and three independent experiments were performed. All primer sequences are listed in Table 1.

## 1.6 Immune response of macrophages

### 1.6.1 Culture of macrophages

A murine macrophage cell line (RAW 264.7) was used for comparing Ti-4M-H to Ti and Ti-H. The cells were cultured in DMEM medium supplemented with 10% FBS and 1% penicillin/streptomycin, at 37 °C and 5% CO<sub>2</sub> in a humidified environment.

### 1.6.2 Cell adhesion and viability

The morphology and immunofluorescence staining of macrophages on samples was observed by FE-SEM after culturing for 24 h. Cell proliferation was measured using the CCK8 assay (Beyotime) using the same procedures as described in Section 1.5.3.

### 1.6.3 Cell polarization

Cells were seeded onto samples and cultured for 6 or 12 days, after which they were pretreated with 0.1% EDTA solution and resuspended using a cell scraper. Protein analysis for macrophage polarization was performed using flow cytometry (Quanta SC, Beckman Coulter, USA) with antibodies (Abcam, Cambridge, UK) specific for markers of the M1 (CCR7) and M2 (CD206) phenotypes. The mean fluorescence intensity (MFI) for M1 and M2 markers were also calculated and analyzed.

#### 1.6.4 Inflammation-related gene expression

The expression levels of inflammation-related genes (TNF- $\alpha$ , Arg-1, IL-1 $\beta$ , TGF- $\beta$ 1, IL-10, IL-6, and iNOS) were determined using real-time RT-PCR using the same procedures as described in Section 1.5.5. All primer sequences are listed in Table 1.

#### 1.7 Cross talk between macrophages and osteoblasts

##### 1.7.1 Effects of osteoblasts on macrophages

MC3T3 osteoblast cells were cultured on Ti, Ti-H and Ti-4M-H samples for 24 hours, after which cells were digested and the culture medium was collected. The cell-suspended medium was centrifuged at 5000 rpm for 10 min to remove cells. This supernatant medium was mixed with fresh DMEM medium in a 1:1 ratio to make osteoblast-conditioned medium (CM 1). RAW 264.7 macrophages were cultured in CM 1 for 3 and 7 days, after which RT-PCR was used to analyze inflammation-related gene expression.

##### 1.7.2 The effect of macrophages on osteoblasts

RAW 264.7 macrophages were cultured on Ti, Ti-H and Ti-4M-H samples for 24 hours, after which cells were digested and the culture medium was collected. The cell-suspended medium was centrifuged at 5000 rpm for 10 min to remove cells. This supernatant medium was mixed with fresh DMEM medium in a 1:1 ratio to make macrophage-conditioned medium (CM 2). MC3T3 osteoblasts were cultured in CM 2 for 3 and 7 days, after which RT-PCR was used to analyze osteogenesis-related gene expression.

#### 1.8 *In vivo* experiments

##### 1.8.1 Animals and surgical procedures

Animal studies were approved by the Tab of Laboratory Animal Ethical Inspection, School of Stomatology, Fourth Military Medical University prior to the onset of the experiments (Xi'an,

China; IRB approval number: 2019(085); date: July 18, 2019). All animal experiments were carried out in compliance with the policy of Fourth Military Medical University on animal use and ethics. All animal care was conducted with full consideration of animal welfare. A total of 36 male adult Sprague-Dawley rats aged 12 weeks and weighing 250-300 g (supplied by the Fourth Military Medical University) were used in this study. The rats underwent general anesthesia with sodium pentobarbital (30 mg/kg, MerckDrugs & Biotechnology, Germany) through intraperitoneal injection before implant surgery. The bone surface of the tibia was exposed by incising the skin and muscles. The implant (Ti, Ti-H or Ti-4M-H) was inserted completely into the tibial marrow cavity, and the wound was sutured in layers. After the operation, antibiotics (ampicillin, 12.5 mg/kg) were administered for 7 days to prevent infection. At each harvesting time (2 weeks post-surgery for macrophage detection or 12 weeks post-surgery for bone mass detection), all animals were sacrificed by a lethal dose of anesthesia. The tibial samples containing implants were harvested and fixed in 4% paraformaldehyde for the following analyses.

### 1.8.2 Micro-computed tomography scanning

Micro-computed tomography ( $\mu$ -CT) was used to image the explanted samples (Y. Cheetah, Y. XLON; parameter settings: 90 kV, 45  $\mu$ A, 1000-ms; isotropic voxel size: 17  $\mu$ m). The region of interest was set as the cancellous bone and the distance within 200  $\mu$ m of the implant surface. Reconstructed 3D images were used to calculate the bone volume/total volume (BV/TV).

### 1.8.3 Immunohistochemical staining

After micro-CT scanning, samples were decalcified in 10% EDTA for 3 weeks, after which the implants were easily removed from the tibia. After sequential dehydration using a graded ethanol series, samples were embedded in paraffin and sectioned with a thickness of 4  $\mu$ m, followed by immunohistochemical staining for iNOS (Abcam) and Arg (Santa Cruz



Biotechnology Inc., Dallas, TX, USA). Fluorescence of Inos and Arg were measured and quantified using the digitized image analysis (Leica).

#### 1.8.4 Double fluorescence labeling of tetracycline-calcein staining

Animals requiring tetracycline-calcein double fluorescence labeling were injected intraperitoneally with tetracycline (25 mg/kg) and calcein (5 mg/kg) for **at** 13 and 3 days before sacrifice, respectively. Following sacrifice, the samples were fixed with 75% alcohol for one week protected from light. Tissue embedding without decalcification was performed, and sections with a thickness of 50  $\mu\text{m}$  were obtained. Fluorescence labeling in the bone surrounding the implant was observed using a fluorescence microscope. Yellow fluorescence indicated bone tissue labeled with tetracycline, representing bone mineralization at 13 days prior to sacrifice, while green fluorescence indicated bone tissue labeled with calcein, representing bone mineralization at 3 days prior to sacrifice. The distance between the yellow (①) and green (②) bands indicated the amount of bone mineralization around the implant that formed within a one-week period. This allowed quantitative analysis where bone mineralization deposition rate (MAR,  $\mu\text{m}/\text{d}$ ) = the distance between the two bands / marking interval period.

#### 1.8.5 Histological analysis

The 50  $\mu\text{m}$  thick sections were stained using Masson's trichrome to evaluate the extent of bone-implant contact, which was defined as the ratio of contact length between bone tissue and implant to the total implant length.

### 1.8.6 Biomechanical test

Immediately after harvest, samples of each group were tested and recorded to subjected to the maximal pull-out force, using a universal material testing system (AGS-10KNG; Shimadzu, Kyoto, Japan) with a compression speed of 2 mm/min.

### 1.9 Statistical analysis

Statistical analysis was performed using SPSS 17.0, and all data were expressed as mean  $\pm$  standard deviation. Levene's test was performed to determine the homogeneity of variance for all data. Tukey HSD post hoc tests were used for data with homogeneous variance. Tamhane's T2 post hoc test was used for test groups without a homogeneous variance. A p-value of less than 0.05 was considered significant.

**Table 1** Primer sequences for real-time RT-PCR

Gene	Sequences(5'-3')
Runx-2	F:ATCCAGCCACCTTCACTTACACC
	R:GGGACCATTGGGAAGTATAGG
ALP	F:TATGTCTGGA ACCGCACTGAAC
	R:CACTAGCAAGAAGAAGCCTTTGG
OPN	F:GACGGCCGAGGTGATAGCTT
	R:CATGGCTGGTCTTCCCGTTGC
OCN	F:GCCCTGACTGCATTCTGCCTCT
	R:TCACCACCTTACTGCCCTCCTG
GAPDH	F:GGCACAGTCAAGGCTGAGAATG
	R:ATGGTGGTGAAGACGCCAGTA
VEGF	F:AAGTGTGCGACCCCAAATTC'
	R:ACCATCCCCTGTCTGTCTG

OSM	F:AACTCTTCCTCTCAGCTCCT R:TGTGTTTCAGGTTTTGGAGGC
BMP2	F:GGGACCCGCTGTCTTCTAGT R:TCAACTCAAATTCGCTGAGGAC
CCL2	F:CCCACTCACCTGCTGCTACT R:TCTGGACCCATTCCTTCTTG
iNOS	F:TCTCAAACCTGCTCTGAGGTG R:CGTTGGATTTGGAGCAGAAGTG
TNF- $\alpha$	F:GCCACCACGCTCTTCTGTCT R:GGTCTGGGCCATAGAACTGATG
IL-1	F:AACCTGCTGGTGTGTGACGTC R:CAGCACGAGGCTTTTTTGTGT
Arg-1	F:CTCCAAGCCAAAGTCCTTAGAG R:AGGAGCTGTCA-TTAGGGACATC
IL-10	F:GCCAGAGCCACATGCTCCTA R:GATAAGGCTTGGCAACCCAAGTAA
TGF- $\beta$	F:TAATCGTGAATCAGGCAG R:ATCCATCACTAGATCGCCCT
IL-6	F:CCAGAAACCGCTATGAAGTTCCT R:CACCAGCATCAGTCCCAAG
$\beta$ -actin	F:GGCAGTGTTTTGGGCATATTC R:GATGACGATATCGCTGCGCTG

---

## 2. Supplementary Results

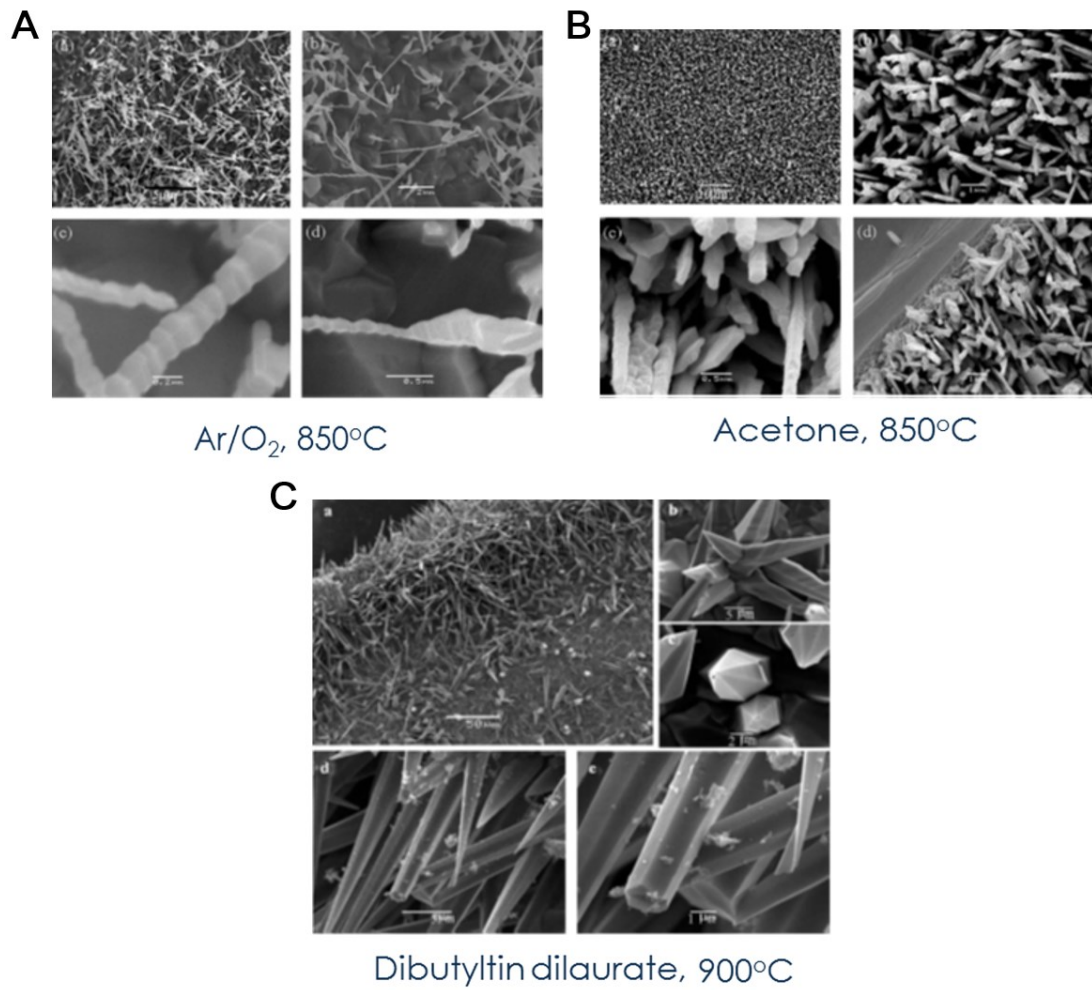


Figure S1. SEM images of Ti6Al4V calcined in Ar/O<sub>2</sub> (A), acetone atmosphere at 850 °C, 1 h (B)<sup>[5]</sup>, and dibutyltin dilaurate atmosphere at 900 °C, 1 h (C)<sup>[6]</sup>.

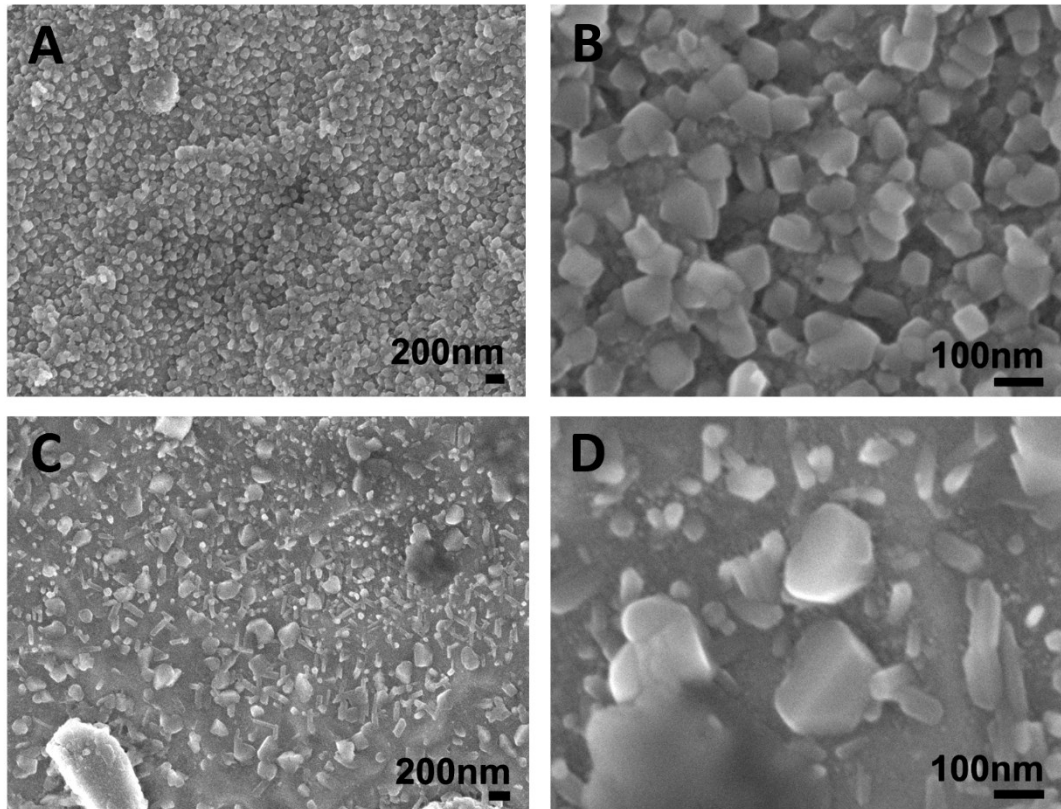


Figure S2. SEM images of Ti6Al4V (A, B) and APD-treated Ti6Al4V subjected to thermal annealing at 600 °C for 1 h (C, D).

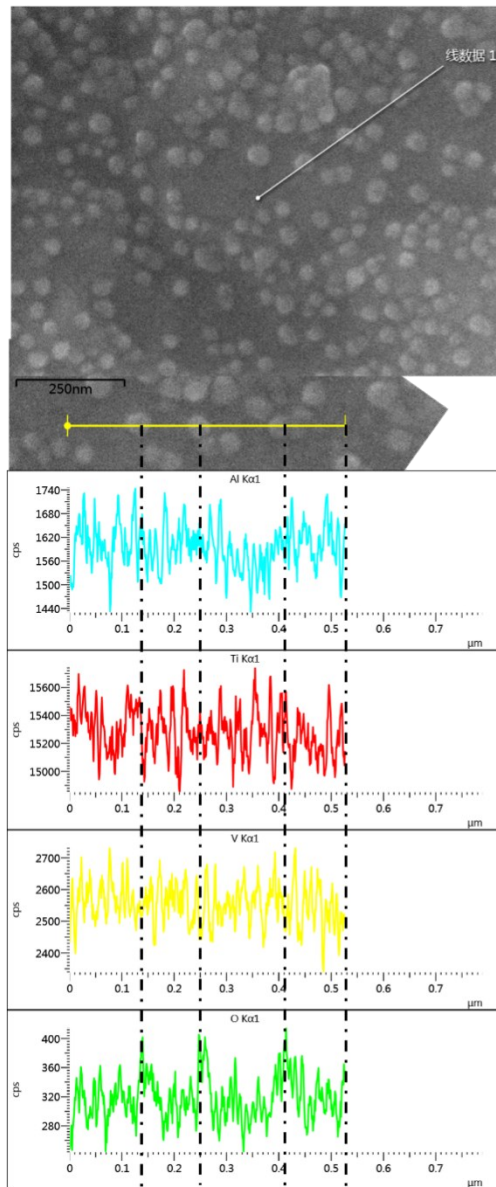


Figure S3. SEM images and EDS line-scan of Ti-4M-H.

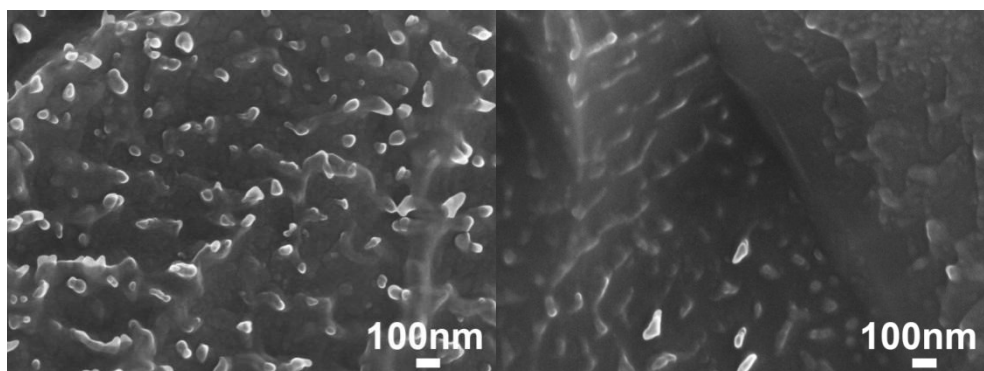


Figure S4. SEM images of APD-treated Ti6Al4V samples annealed in an Ar atmosphere at 500 °C for 1 h.

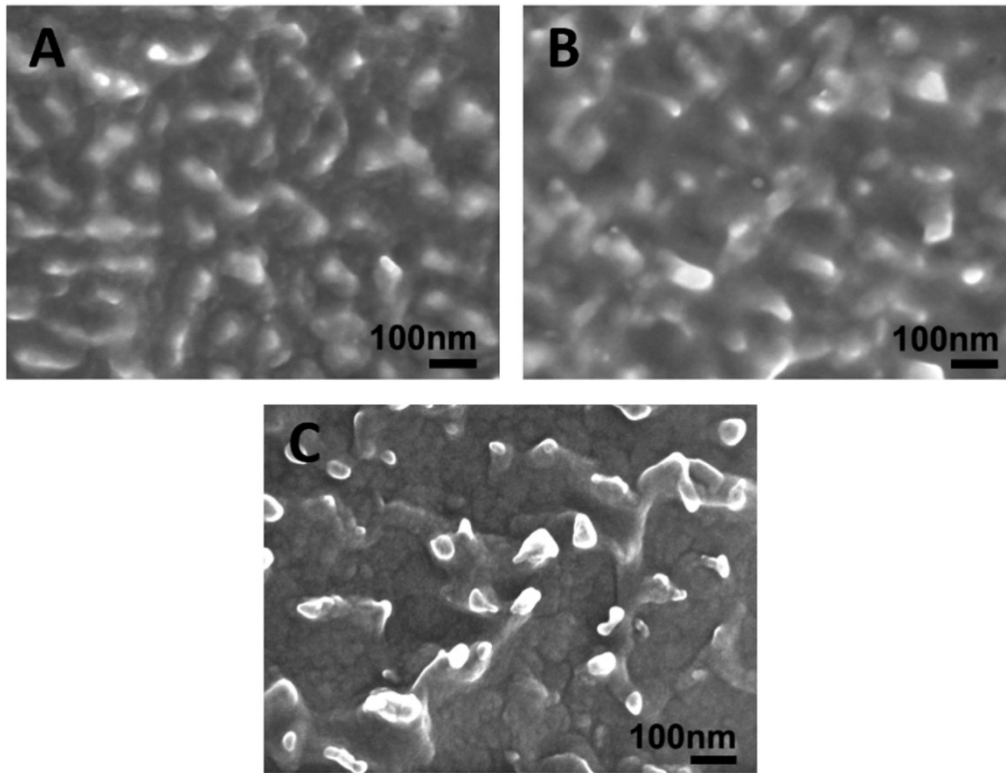


Figure S5. SEM images of APD-treated Ti6Al4V samples subjected to annealing at 350 °C for 1 h (A), 400 °C for 1 h (B), and 500 °C for 30 min (C).

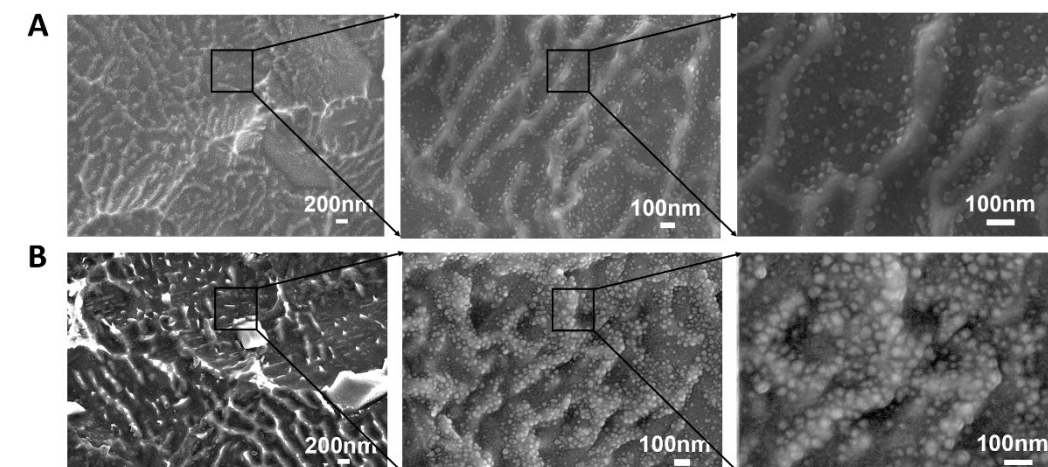


Figure S6. SEM images of Ti6Al4V treated by NaOH-induced AAD (A), and AAD based film deposition of Ti (B). A thin layer of Ti film was deposited by electron beam evaporation on the sample surface (Ti-evp Ti), which was then subjected to thermal annealing (Ti-evp Ti-H).

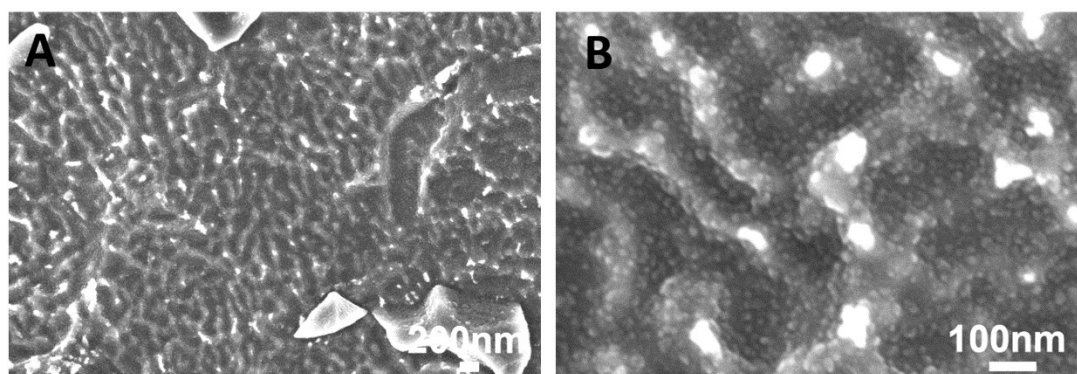


Figure S7. SEM images of APD-treated Ti6Al4V samples washed with diluted hydrochloric acid solution and then thermally annealed at 500 °C for 1 h.

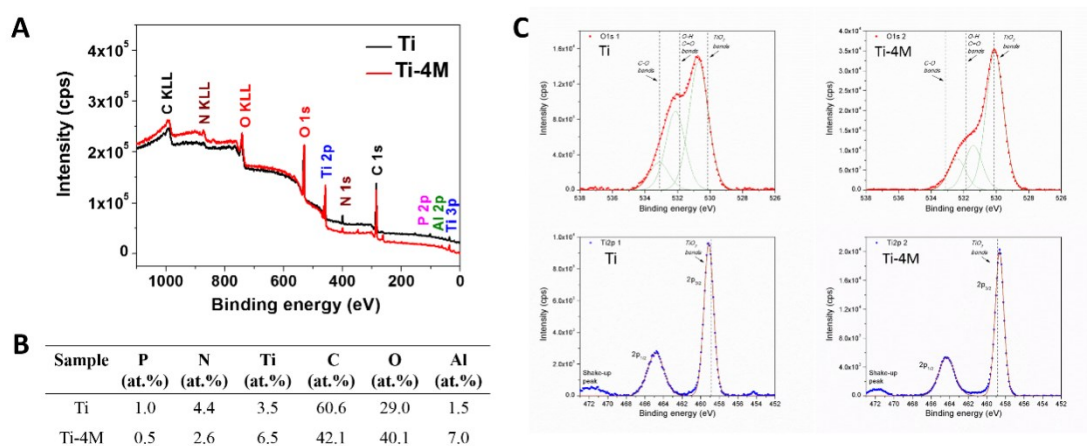


Figure S8. XPS survey spectra of the Ti and Ti-4M (A), their quantitative elemental composition (B), and the fitting spectra of O1s and Ti2p (C).



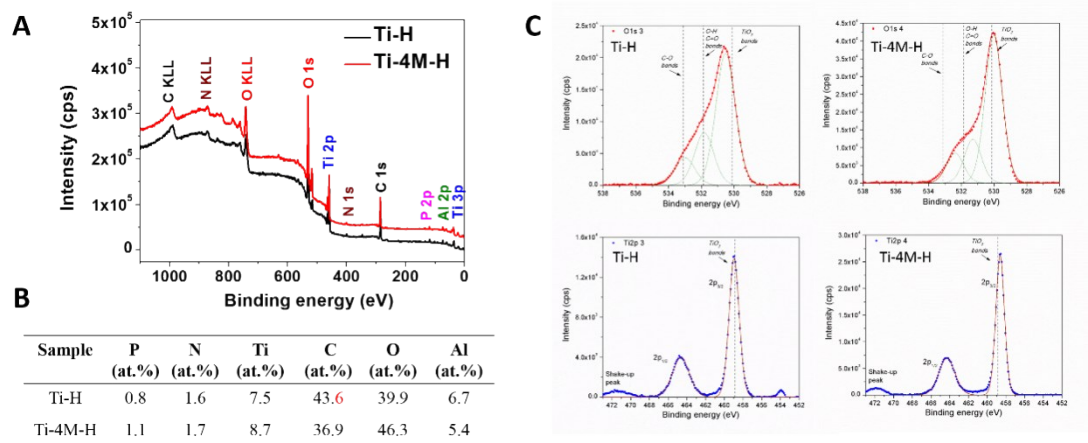


Figure S9. XPS survey spectra of the Ti-H and Ti-4M-H (A), their quantitative elemental composition (B), and the fitting spectra of O1s and Ti2p (C).

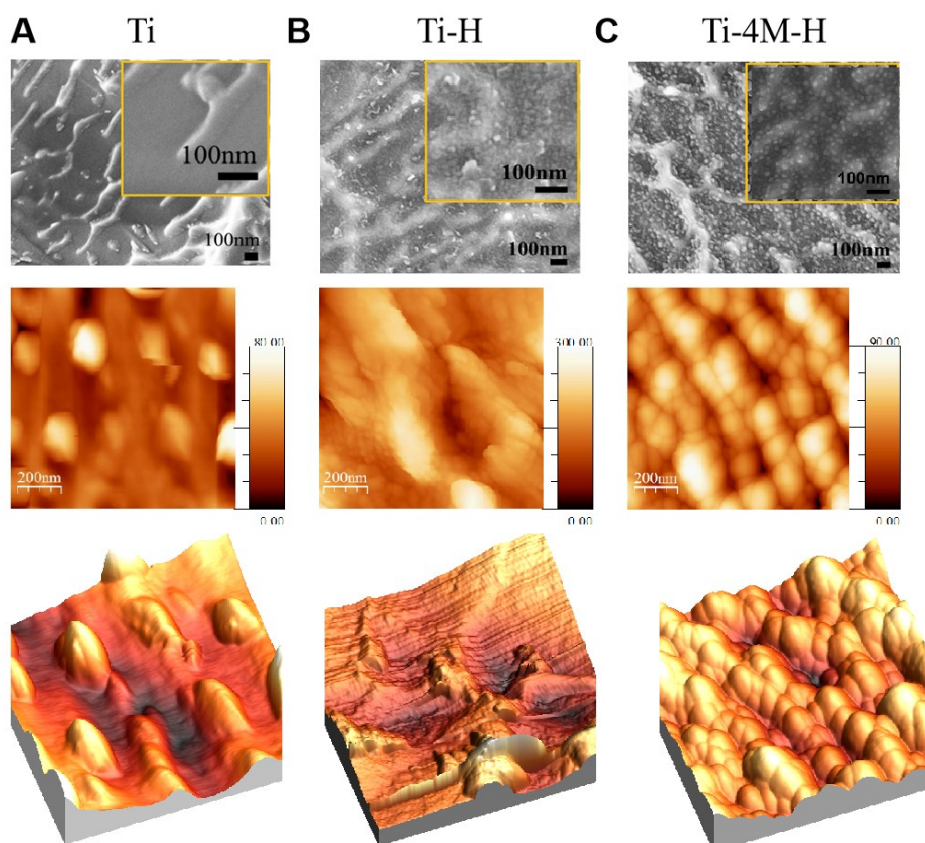


Figure S10. SEM (top panel), two dimensional (2D; middle panel) and three dimensional (3D; bottom panel) AFM images of Ti (A), Ti-H (B) and Ti-4M-H (C).

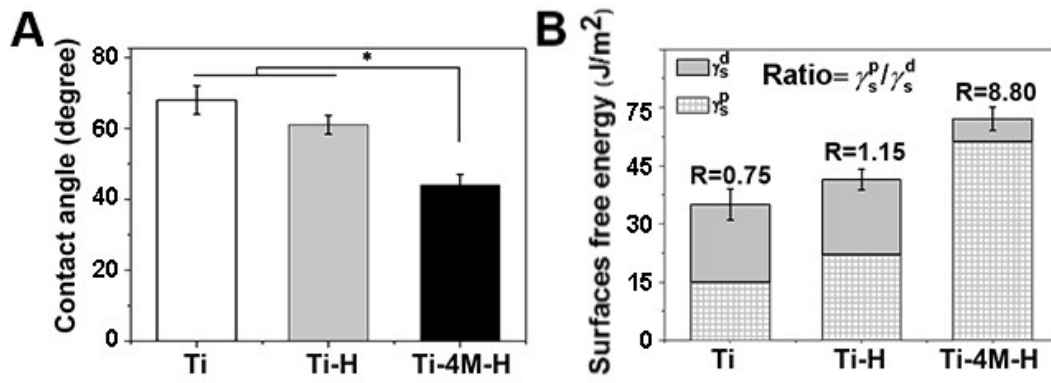


Figure S11. Contact angle (A) and surface free energy (B) of Ti, Ti-H and Ti-4M-H.  $\gamma_s^d$ : dispersive solid surface tension;  $\gamma_s^p$ : polar solid surface tension. Ratio values ( $\gamma_s^d / \gamma_s^p$ ) are marked on the bars.

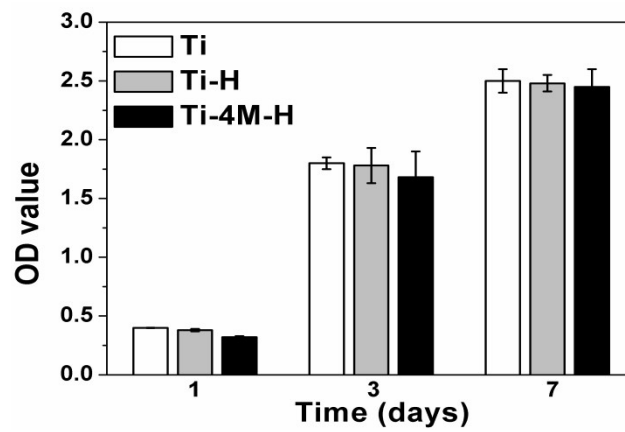


Figure S12. Proliferation of RAW 264.7 cells on sample groups detected by CCK-8 assay.

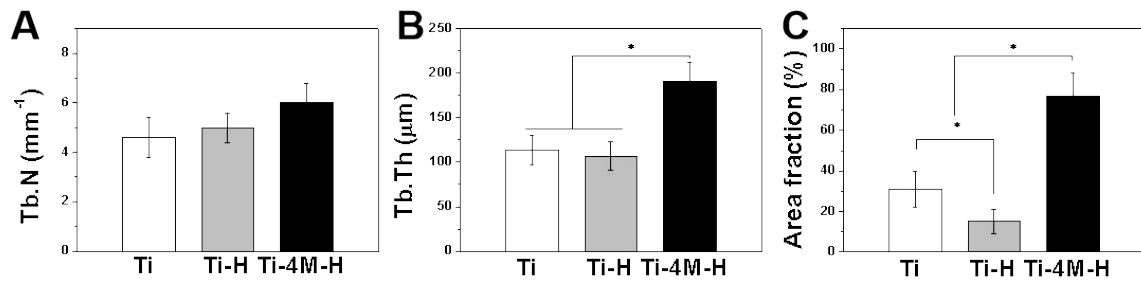


Figure S13. Quantitative histograms of bone formation. Tb.Th: Trabecular Thickness (A), (B) Tb.N: trabecular number (A), Tb.Th: trabecular thickness (B), and the area fraction of mineralized bone (C). \* $p < 0.05$ .

## References

- [1] C. Della Volpe, D. Maniglio, M. Brugnara, S. Siboni, M. Morra, *J. Colloid Interface Sci.* **2004**, 271, 434.
- [2] D. K. Owens, R. C. Wendt, *J. Appl. Polym. Sci.* **1969**, 13, 1741.
- [3] P. E. Luner, E. Oh, *Colloids Surfaces A Physicochem. Eng. Asp.* **2001**, 181, 31.
- [4] C.-C. Liang, A. Y. Park, J.-L. Guan, *Nat. Protoc.* **2007**, 2, 329.
- [5] X. Peng, A. Chen, *J. Mater. Chem.* **2004**, 14, 2542.
- [6] X. Peng, A. Chen, *Appl. Phys. A* **2005**, 80, 473.